

## Flow Quality for Turbine Engine Loads Simulator (TELS) Facility

R. J. Schulz  
ARO, Inc.

June 1980

Final Report for Period October 1, 1978 — September 1, 1979

Approved for public release; distribution unlimited

ARNOLD ENGINEERING DEVELOPMENT CENTER  
ARNOLD AIR FORCE STATION, TENNESSEE  
AIR FORCE SYSTEMS COMMAND  
UNITED STATES AIR FORCE

## NOTICES

When U. S. Government drawings, specifications, or other data are used for any purpose other than a definitely related Government procurement operation, the Government thereby incurs no responsibility nor any obligation whatsoever, and the fact that the Government may have formulated, furnished, or in any way supplied the said drawings, specifications, or other data, is not to be regarded by implication or otherwise, or in any manner licensing the holder or any other person or corporation, or conveying any rights or permission to manufacture, use, or sell any patented invention that may in any way be related thereto.

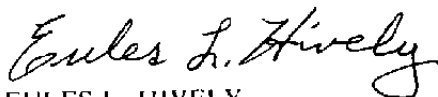
Qualified users may obtain copies of this report from the Defense Technical Information Center.

References to named commercial products in this report are not to be considered in any sense as an indorsement of the product by the United States Air Force or the Government.

This report has been reviewed by the Office of Public Affairs (PA) and is releasable to the National Technical Information Service (NTIS). At NTIS, it will be available to the general public, including foreign nations.

## APPROVAL STATEMENT

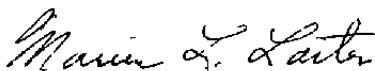
This report has been reviewed and approved.



EULES L. HIVELY  
Project Manager  
Directorate of Technology

Approved for publication:

FOR THE COMMANDER



MARION L. LASTER  
Director of Technology  
Deputy for Operations

# UNCLASSIFIED

REPORT DOCUMENTATION PAGE		READ INSTRUCTIONS BEFORE COMPLETING FORM
1. REPORT NUMBER <b>AEDC-TR-79-83</b>	2. GOVT ACCESSION NO.	3. RECIPIENT'S CATALOG NUMBER
4. TITLE (and Subtitle) <b>FLOW QUALITY FOR TURBINE ENGINE LOADS SIMULATOR (TELS) FACILITY</b>		5. TYPE OF REPORT & PERIOD COVERED <b>Final Report - October 1, 1978 to September 1, 1979</b>
		6. PERFORMING ORG. REPORT NUMBER
7. AUTHOR(s) <b>R. J. Schulz, ARO, Inc., a Sverdrup Corporation Company</b>		8. CONTRACT OR GRANT NUMBER(s)
9. PERFORMING ORGANIZATION NAME AND ADDRESS <b>Arnold Engineering Development Center/ DOT Air Force Systems Command Arnold Air Force Station, Tennessee 37389</b>		10. PROGRAM ELEMENT, PROJECT, TASK AREA & WORK UNIT NUMBERS <b>Program Element 65807F</b>
11. CONTROLLING OFFICE NAME AND ADDRESS <b>Arnold Engineering Development Center/DOS Air Force Systems Command Arnold Air Force Station, Tennessee 37389</b>		12. REPORT DATE <b>June 1980</b>
		13. NUMBER OF PAGES <b>39</b>
14. MONITORING AGENCY NAME & ADDRESS (if different from Controlling Office)		15. SECURITY CLASS (of this report)  <b>UNCLASSIFIED</b>
		15a. DECLASSIFICATION/DOWNGRADING SCHEDULE <b>N/A</b>
16. DISTRIBUTION STATEMENT (of this Report)  <b>Approved for public release: distribution unlimited.</b>		
17. DISTRIBUTION STATEMENT (of the abstract entered in Block 20, if different from Report)		
18. SUPPLEMENTARY NOTES  <b>Available in Defense Technical Information Center (DTIC)</b>		
19. KEY WORDS (Continue on reverse side if necessary and identify by block number) <div style="display: flex; flex-wrap: wrap;"> <div style="width: 33%;">inlets</div> <div style="width: 33%;">cross flow</div> <div style="width: 33%;">mathematical prediction</div> <div style="width: 33%;">gas turbines</div> <div style="width: 33%;">exhaust gases</div> <div style="width: 33%;">nonuniform flow</div> <div style="width: 33%;">loads</div> <div style="width: 33%;">ingestion (engines)</div> <div style="width: 33%;">simulators</div> <div style="width: 33%;">difference equations</div> <div style="width: 33%;">flow separation</div> <div style="width: 33%;">mathematical models</div> </div>		
20. ABSTRACT (Continue on reverse side if necessary and identify by block number) <p>A study was made to define the flow quality in air inlets used to support engine testing in the proposed Turbine Engine Loads Simulator Facility (TELS). The study showed that inlets could be designed that would produce separation-free flow for the worst case of crossflow induced by TELS rotation. The severity of recirculated exhaust gas ingestion by the inlet was estimated using a finite-difference numerical simulation of the</p>		

# UNCLASSIFIED

## UNCLASSIFIED

### 20. ABSTRACT (Continued)

engine and its exhaust deflector. Finally, a method was devised for defining the performance of a representative engine, the Pratt and Whitney F100 engine; the possible effects of inlet flow nonuniformity on engine performance in TELS were detailed.

UNCLASSIFIED

## **PREFACE**

The work reported herein was conducted by the Arnold Engineering Development Center (AEDC), Air Force Systems Command (AFSC). The results were obtained by ARO, Inc., AEDC Division (a Sverdrup Corporation Company), operating contractor for the AEDC, AFSC, Arnold Air Force Station, Tennessee, under ARO Project Numbers E32C-04 and E32C-04A. The Air Force project manager was Mr. Eules L. Hively. The manuscript was submitted for publication on September 28, 1979.

## CONTENTS

	<u>Page</u>
1.0 INTRODUCTION . . . . .	5
2.0 ANALYSIS	
2.1 Flow Simulation . . . . .	5
2.2 Gas Ingestion . . . . .	7
2.3 Distortion Indices and Engine Mathematical Models . . . . .	9
3.0 CONCLUSIONS AND RECOMMENDATIONS . . . . .	11
REFERENCES . . . . .	11

## ILLUSTRATIONS

### Figure

1. Preliminary Engineering Concept of TELS . . . . .	13
2. Candidate Inlet Designs . . . . .	14
3. Approximate Streamline Pattern Into Flared Bellmouth Inlet, No Inlet Separation . . . . .	17
4. Lines of Isovelocity in Meridional Cross Section of Flared Inlet Showing Nonuniformity of Velocity Field . . . . .	18
5. Schematic of Engine and Deflector Simulation . . . . .	21
6. Theoretical Flow Fields Around the TELS Engine-Exhaust Deflector System . . . . .	22
7. Isotherms around the Engine-Exhaust Deflector System . . . . .	25
8. Models of Exhaust Gas Deflectors . . . . .	26

## TABLE

1. Engine Mathematical Models at AEDC . . . . .	27
---	----

## APPENDIX

A. COMPUTATIONS OF EXHAUST GAS INGESTION BY ENGINE IN TELS . . . . .	29
NOMENCLATURE . . . . .	36

## 1.0 INTRODUCTION

In order that measurements can be made of structural and aeromechanical turbine engine behavior, it is imperative that there exist a turbine engine test facility capable of simulating flight-maneuver-induced gyroscopic and inertial loadings on operating gas turbine engines (Refs. 1 through 4). The requirements for such testing have been defined, and a test facility has been described that would meet these objectives. A preliminary design concept of this facility, called the Turbine Engine Loads Simulator Facility (TELS), is shown in Fig. 1. The facility is a large, rotating arm with a variable-position engine mounting structure and counterweight. The arm is of a truss-like structural configuration and is about 40 ft long from the engine centerline (most extended position) to the center of rotation. It is designed to rotate at angular speeds of up to 3.5 radians/sec. The engine support structure also supports and positions the X-ray radiograph monitoring system, which evaluates engine structural deflections or motions during imposed-loadings.

To operate properly, test engines must ingest air of adequate flow quality. Air entering the engine compressor and fan must have acceptably low total-pressure and total-temperature spatial distortions or nonuniformities. For these conditions to exist, the engine inlet must operate unstalled or unseparated, and the jet thrust deflector must direct hot exhaust gases away from the engine inlet. These conditions must be incorporated into the design of the TELS facility so that routine loads testing can be satisfactorily performed with the engine running reasonably close to actual flight maneuvers operating points.

The objective of the present investigation and analysis was to assess inlet flow quality for turbine engine operation in TELS by evaluating inlet and jet deflector performance in crossflows. Another objective was to devise a method for predicting engine performance subject to the predicted inlet flow quality.

## 2.0 ANALYSIS

### 2.1 FLOW SIMULATION

A survey of crossflow/crosswind effects on gas turbine engine inlets established that an extensive and thorough study of inlet behavior is being performed by researchers at the NASA Lewis Research Center, Cleveland, Ohio. The main thrust of the NASA research lies in the design and development of inlets for V/STOL aircraft applications. One important product of this research program has been the development of technology for predicting three-dimensional potential flow in plane or in axisymmetric inlets subject to uniform but arbitrarily directed crossflow. This technology and its applications for interpreting inlet behavior in crosswinds/crossflows are described in Refs. 5 through 11.

Another aspect of this technology for inlet evaluation is the development and use of a modern finite-difference boundary-layer solution procedures (Ref. 12) to identify flow-separation events in inlets. Thus, once the potential main or bulk inlet flow field has been found, then the viscous behavior of the flow in inlets can be predicted, based on boundary-layer theory.

The technology necessary to evaluate inlet behavior in crossflows was obtained from N. O. Stockman of NASA Lewis Research Center. The system was made operational at AEDC by G. W. Lewis, ARO, Inc. In addition, Lewis added computer-plot subroutines for displaying longitudinal and traverse contours of constant velocity and static pressure. A set of inlet designs was selected for evaluation; these designs covered the normal range of inlet configurations currently available for crosswind engine testing. Three geometries from this set are shown in Fig. 2. The compressor face was a model of the F100 engine configuration. The flow fields were calculated for the worst case of crossflow,  $V_{\infty} = 140$  ft/sec. This cross-flow maximum velocity corresponds to the tip velocity of the TELS arm at an angular velocity of 3.5 radians/sec. The angle of attack of the inlet for the worst-case condition corresponds to 90 deg, the vertical engine position shown in Fig. 1.

The calculations provided (1) the spatial location of the stagnation lines in and around the inlets, (2) the general, three-dimensional velocity field over the inlet configuration, and (3) the flow inside the inlet up to the simulated compressor face station. A boundary-layer analysis of the potential flow field revealed unsatisfactory performance of the first two inlet designs, A and B (Fig. 2). The flow separated from the forward or upstream lip of these geometries in the meridional or symmetry plane. For the third geometry design, C (Fig. 2), the boundary-layer analysis indicated no flow separation or stall. Hence, this wide, flared-bellmouth design would operate unstalled for the worst case of TELS crossflows. The free-stream, inlet streamline pattern is shown schematically in Fig. 3. Figure 3 shows a section of the three-dimensional stream tubes, a view in the plane of the cross-flow velocity. The indicated stagnation points are points on stagnation streamlines. In the meridional plane the rear stagnation point lies on the inner edge of the flared lip. This may indicate a possible problem with flow stability; calculations made with the computer simulation showed this stagnation point location to be sensitive to variations in engine airflow rates and crossflow velocity.

This flared-bellmouth geometry is only one example of the geometries that would produce acceptable flow quality, and it may not necessarily represent the best design. An optimization of the inlet design may be performed in future studies using these computational tools. Measures of quality to be optimized are discussed in Section 3.0.

The qualitative nature of the unstalled velocity field in the flared inlet is shown in Fig. 4. The calculated potential flow field was interpolated to provide contour plots of constant total velocity magnitude, axial velocity component, and radial velocity component. The velocity field is not symmetrical about the centerline, indicating that a distorted static-pressure field will exit in the inlet. However, data exist showing that this may not adversely affect engine performance.

In Ref. 13, a turbofan engine with an asymmetric inlet was tested at high crossflow velocities (up to 160 knots) and large angles of attack (up to 120 deg). The engine operated satisfactorily without flow separation at conditions even severer than the worst case of TELS. Though asymmetric, the inlet looked quite similar to inlet B in Fig. 2, but it had a thicker tip facing the crossflow direction. Thus, it appears that the presence of the engine can considerably reduce inlet separation, compared to analytic predictions, and can handle distorted velocity in static pressure fields reasonably well.

## 2.2 GAS INGESTION

A mathematical simulation of the turbojet engine and jet deflector was formulated to estimate the severity of the recirculating exhaust gas ingestion problem. The simulation was developed as a two-dimensional, finite-difference model of a turbojet engine and an exhaust gas deflector. The computational mesh encompassed the surrounding flow field far enough upstream and downstream of the engine to simulate the undisturbed far-field upstream and a "fully developed" downstream condition. (However, an actual three-dimensional flow will not reach a fully developed state but dispersed in some manner depending on the shifting of the wind over the existing terrain.) The fully developed flow condition is a useful mathematical boundary condition. The undisturbed free stream (far above the engine) and the ground plane formed the other boundaries of the simulation. Figure 5 gives the model, the mesh spacing system, and the lengths incorporated in the simulation.

The crossflow interaction with the deflected exhaust jet and the engine inlet flow was computed in this mesh system by a finite-difference solution of the full, elliptic, Navier-Stokes and energy equations subject to imposed boundary conditions. In this study, the effects of compressibility were neglected. However, the solution procedure written included a Poisson-type equation for the static pressure that may be solved simultaneously with the other field equations. The finite-difference solution procedure was used in a limited parametric study of various effects on the severity of engine inlet ingestion of hot exhaust gases. The present study was limited to an investigation of the effects of crosswind velocity at a constant turbulent viscosity level on gas ingestion for a fixed-geometry, flat-plate jet deflector. Although the deflector geometry was flat, curved deflectors can be simulated using different boundary conditions along the deflector surface.

The velocity and temperature distributions shown in Fig. 6 are typical results of the present numerical investigation. In this case a sine function was used to describe the deflector boundary conditions. (The actual distribution is provided in Sections A6.0 and A7.0 of the appendix). These results show no significant gas ingestion problem in the engine inlet plane. The temperature of the gas entering the inlet is only slightly higher ( $10^{\circ}\text{R}$ ) than the free-stream temperature of and at a uniform spatial profile. Figure 7 shows isotherms in the flow in the engine tailpipe vicinity. The flat plate is assumed to rise to the exhaust gas temperature; thus, the flow above the deflector is hot. Obviously, sensitive instrumentation should not be placed aft of or in the wake of the deflector.

The value of the Reynolds number selected for this flow was much lower than that normally used for turbulent mixing based on simple jet mixing theory. The lower number was used in order to account for the turbulence created by the rotation of the TELS arm. The arm can be expected to cause a local, well-mixed crossflow of extremely high turbulence and hence high effective viscosity. Calculations were made with values of turbulent Reynolds number an order-of-magnitude higher than those displayed in Figs. 6 and 7, and, though the velocity and the temperature fields changed, the inlet temperature profiles remained essentially flat. Similar results were obtained for calculations performed for crossflow velocities ranging from 25 to 140 ft/sec.

The analysis carried out in this study suggests that with a careful design of engine mounting structures, there is little chance of exhaust gas ingestion for test cases that use flat-plate-type deflectors located behind a vertically mounted engine in a uniform crossflow velocity. The analysis provides a framework for investigation of other parameters affecting gas ingestion problems. Future work will require investigation of the following problem areas:

1. engine orientation in crossflow,
2. deflector geometry (i.e., such geometries as bucket, angled plate, or splitter plate),
3. turbulence transport model (i.e., in which either one- or two-equation models can be incorporated in the solution procedure),
4. effect of exhaust gas deflector proximity on the exhaust jet static pressure field in engine nozzle exit,
5. buoyancy effects caused by gas temperature variations,
6. three-dimensionality effects, including the scavenging or pumping effect of the rotating TELS arm, and
7. engine exhaust conditions.

The present study neglected the bouyancy effects in the Navier-Stokes equations. This allowed the analysis to provide a "worst-case" description of the flow field since, in actual TELS operation, bouyancy effects would act to lift the hot gases away from the engine inlet. The appropriate source terms are indicated in the Navier-Stokes equations (Appendix A); these terms can be easily incorporated into the solution procedure.

As remarked before, there is a simple method for simulating the effects of other deflector geometries by distributing the velocity profiles along the flat-plate surface. For example, sine or cosine distributions can be defined, with the  $u$  and  $v$  components equal to zero at the deflector plate centerline, but increasing to maximum negative or positive values at the ends of the deflector. This procedure artificially modifies the resultant exhaust jet/deflector flow field. A velocity prediction representing a given deflection geometry may be obtained by first predicting – with a method like that of Ref. 14 – the velocity profiles of the essentially inviscid flow into and out of a given deflector and by then using the exit profiles as the mathematical boundary condition in a program like the one developed for the present study. Figure 8 illustrates this method.

## 2.3 DISTORTION INDICES AND ENGINE MATHEMATICAL MODELS

Work has been done for several years on the formulation and interpretation of gas turbine engine inlet airflow quality. Parameters have been developed whose values correlate with measurable changes in engine behavior. These indices are assigned values by use of mathematical procedures to evaluate engine inlet flow quality. The flow quality is defined theoretically by:

1. the circumferential and radial patterns of steady-state total pressure,
2. the circumferential and radial patterns of steady-state total temperature,
3. swirl strength and distribution,
4. average one-dimensional total pressure fluctuations of "high" (greater than one-per-compressor rotor revolution) and "low" frequency, and
5. average one-dimensional total temperature fluctuations.

The flow quality has not been related either to the velocity or to inlet static pressure fields, but experimentation and a variety of rationale have produced several distortion index parameters. A future standard method for the industry is described in the Society of Automotive Engineers' Aerospace Recommended Practice (ARP) 1420, Ref. 15. The mathematical procedures outlined in this standard are recommended for future calibration or calculation of engine distortion indices. However, each current engine may have indices calculated with procedures unique to that engine. For example,

Table 1 lists the engine mathematical models available at AEDC as recently surveyed by the author. Of these mathematical models, only those for the F100 and F101 engines could account for distortion effects. The F100 engine was selected as representative of the engine type tested in TELS.

The purpose of the present study was not to review these indices but to learn whether such indices existed in mathematical models of engines likely to be tested in TELS and to determine a method for predicting or interpreting engine performance in TELS tests. In carrying out this research it was found that, in addition to the correlation methods for gaging engine performance, both experimental and theoretical studies are in progress to formulate methods for predicting engine response to pressure and temperature perturbations. Compressor models are being formulated and evaluated to gain insight into compressor response to inlet distortion (Refs. 16 and 17).

By using such models to predict engine performance, it may be possible to accurately gage the engine response to inlet flow distortions before TELS testing. Therefore, basically two methods were found for estimating the F100 engine performance in TELS. One method is based on the parallel compressor model for the F100 described by Walter and Shaw (Ref. 17). The other method requires using two computer programs. First, the Pratt and Whitney deck CCD 1087 is used to convert input total pressure and temperature profiles to a set of inlet distortion indices or K-factors. Then, these K-factors are input to the Pratt and Whitney F100-3 engine performance program, deck CCD-1116-3.0, to define the resultant performance. Similar methods are available or can be developed for other current turbine engines.

Some cautionary remarks are needed to qualify the foregoing conclusions. First, data exist that indicate that inlet performance can be improved with an attached engine. The engine has an upstream effect on the flow, not only delaying or minimizing flow separation but also modifying the velocity and static pressure field in the inlet. Therefore, analytical predictions of inlet performance must be cautiously applied when interpreting flows or defining distortion indices for inlets attached to operating turbojet engines. Second, the effects of temperature nonuniformity are twofold. Temperature nonuniformity may affect the aerodynamic behavior of the flow through the compressor by coupling with the pressure field to produce aerodynamic stall, or, in variable-cycle engines, a localized temperature may affect sensors that establish blade or stator angles of attack, thereby causing engine component mismatch. Third, an area of concern for TELS is the interaction of the engine with the inlet flow during engine power-up. Procedures must be devised for accelerating the engine while bringing the TELS facility to speed, without creating transient engine-damaging flow conditions (i.e., those conditions that exist during transient operating procedures that could damage the engine, as opposed to the undamaging, final steady-state conditions).

### 3.0 CONCLUSIONS

An investigation was performed to assess inlet flow quality for turbine engine operation in TELS. First, it was confirmed that an axisymmetric, flared bellmouth operates satisfactorily, i.e., unseparated. Second, a theoretical study of the exhaust gas ingestion in TELS indicates that, for the simple engine/blast deflector arrangement simulated in the study, the gas ingestion problem is insignificant. Third, a method has been devised for evaluating the performance of engines to be tested in TELS. The method is based on the calibrated mathematical engine models that incorporate distortion indices.

### REFERENCES

1. Kinchen, B. E. "Turbine Engine Loads Simulator (TELS) Radiographic Systems Requirements Study." AEDC-TR-77-55 (AD-A040465), June 1977.
2. Mulenburg, G. M. and Mitchell, J. G. "Simulation of Turbine Engine Operational Loads." Presented at the AIAA/SAE 13th Propulsion Conference, Orlando, Florida, July 11 - 13, 1977. AIAA Paper No. 77-912.
3. Swain, R. L. and Mitchell, J. G. "Simulation of Turbine Engine Operational Loads." Journal of Aircraft Vol. 15, No. 6, June 1978.
4. Ryan, J. P. "TELS (Turbine Engine Loads Simulator) Maneuver Profile Development Study." University of Dayton Research Institute Report UDR-78-66, July 1978.
5. Wulf, R. H. "Summary Report for Full Scale Fan Demonstrator Program - Cross-wind Testing." General Electric Report No. R70-AEG-368, September 1970.
6. Stockman, N. O. "Potential and Viscous Flow in VTOL, STOL or CTOL Propulsion System Inlets." Presented at the AIAA/SAE 11th Propulsion Conference, Anaheim, California, September 29 - October 1, 1975. AIAA Paper No. 75-1186.
7. Stockman, N. O. and Farrell, C. A., Jr. "Improved Computer Programs for Calculating Potential Flow in Propulsion System Inlets." NASA TM 73728, July 1977.
8. Boles, M. A., Luidens, R. W., and Stockman, N. O. "Theoretical Flow Characteristics of Inlets for Tilting-Nacelle VTOL Aircraft." NASA TP 1205, E-9387, April 1978.
9. Chou, D. C., Luidens, R. W., and Stockman, N. O. "Prediction of Boundary-Layer Flow Separation in V/STOL Engine Inlets." Journal of Aircraft, Vol. 15, No. 8, August 1978, pp. 474-481.

10. Luidens, R. W., Stockman, N. O., and Diedrich, J. H. "An Approach to Optimum Subsonic Inlet Design." NASA TM 79051, 1979.
11. Hess, J. L. and Stockman, N. O. "An Efficient User-Oriented Method for Calculating Compressible Flow about Three-Dimensional Inlets." Presented at the 17th Aerospace Sciences Meeting, New Orleans, Louisiana, January 15 - 17, 1979. AIAA Paper No. 79-0081.
12. Albers, J. A. and Gregg, J. L. "Computer Program for Calculating Laminar, Transitional, and Turbulent Boundary Layers for a Compressible Axisymmetric Flow." NASA TN D-7521, April 1974.
13. Syberg, J. "Low Speed Test of a High-Bypass-Ratio Propulsion System with an Asymmetric Inlet Designed for Tilt-Nacelle V/STOL Airplane." NASA CR 152072, January 1978.
14. Hiriart Le-Bert, G. "A Theoretical Analysis of Jet Deflection from Plane and Axisymmetric Curved Obstacles." Ph.D. Thesis, Naval Postgraduate School, Monterey, California, December 1973.
15. Turbine Engine Inlet Flow Distortion; Aerospace Recommended Practices (ARP) 1420. Prepared by SAE Committee S-16. March 1978.
16. Mazzawy, R. S. and Banks, G. A. "Circumferential Distortion Modeling of the TF30-P-3 Compression System." NASA CR 135124, January 1977.
17. Walter, W. A. and Shaw, M. "Predicted F100 Engine Response to Circumferential Pressure and Temperature Distortion." Presented at the AIAA/SAE/ASME 15th Joint Propulsion Conference, Las Vegas, Nevada, June 18 - 20, 1979. AIAA Paper No. 79-1310.
18. Roache, P. J. Computational Fluid Dynamics. Hermosa Publishers, Albuquerque, New Mexico, 1972.
19. Chien, J. C. "A General Finite-Difference Formulation with Application to the Navier-Stokes Equations." Journal of Computational Physics, Vol. 20, No. 3, March 1976, pp. 268-278.
20. Schlichting, H. Boundary-Layer Theory. Sixth Edition, J. Kestin, Trans. McGraw-Hill, New York, New York, 1968.

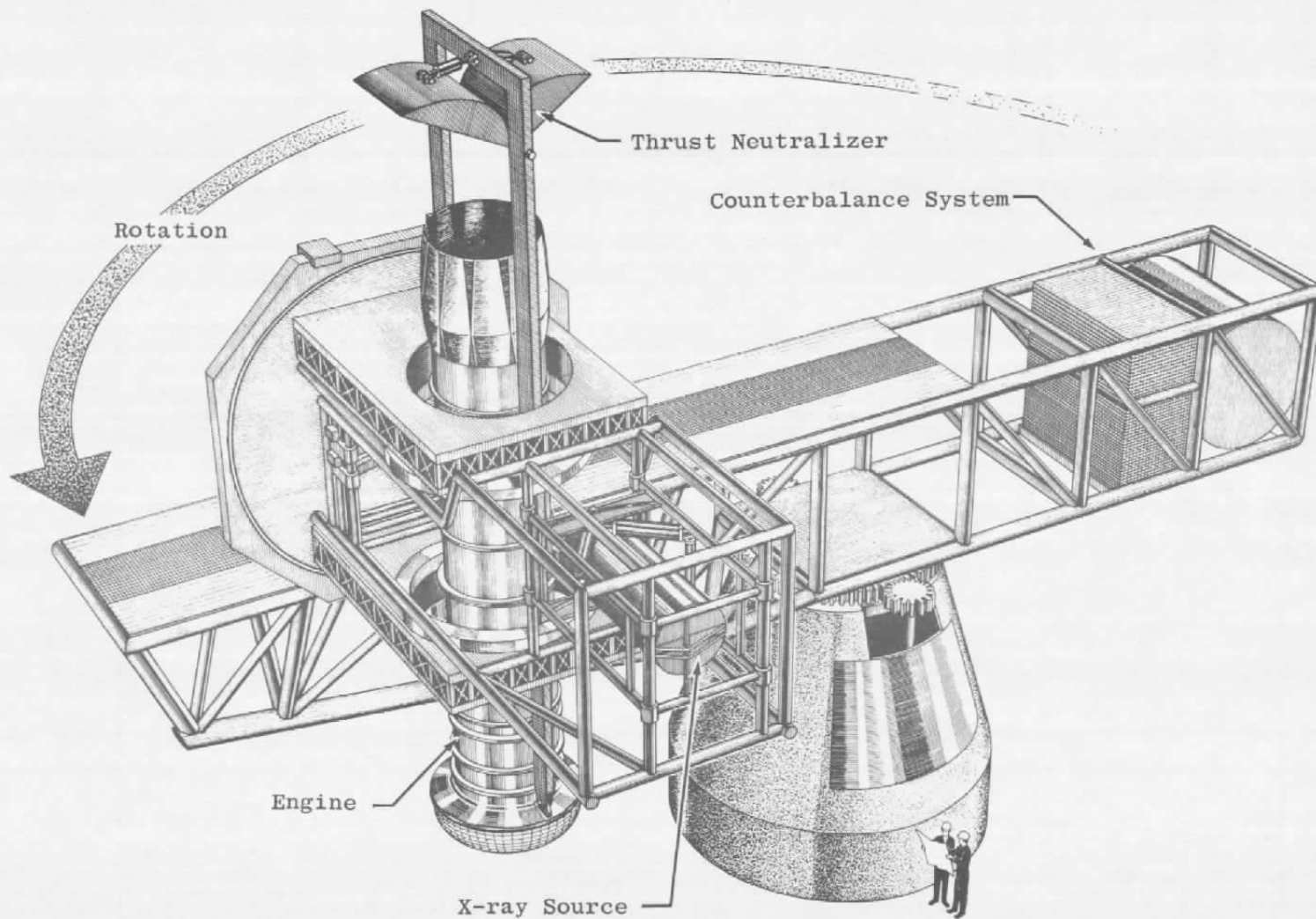
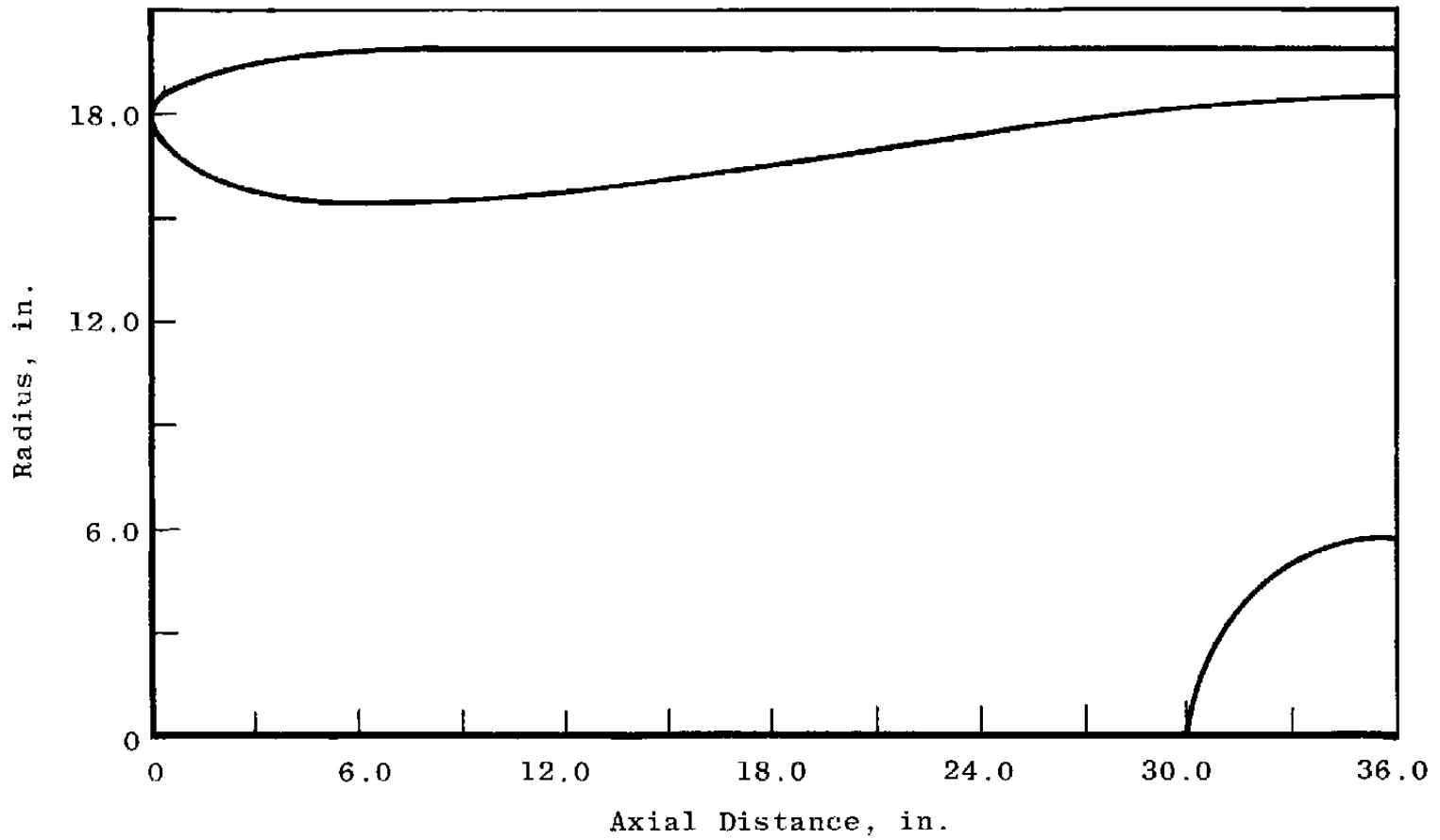
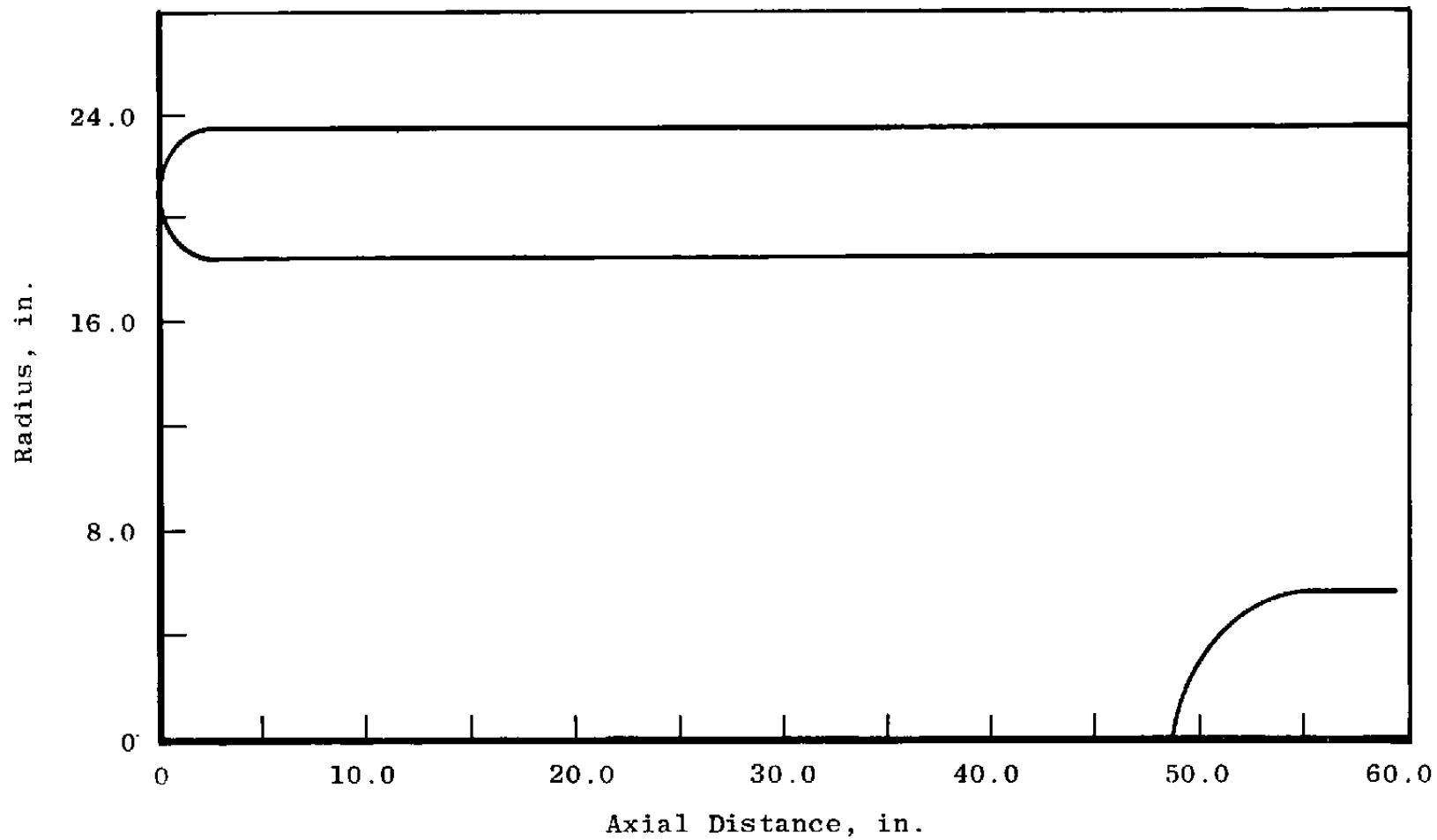


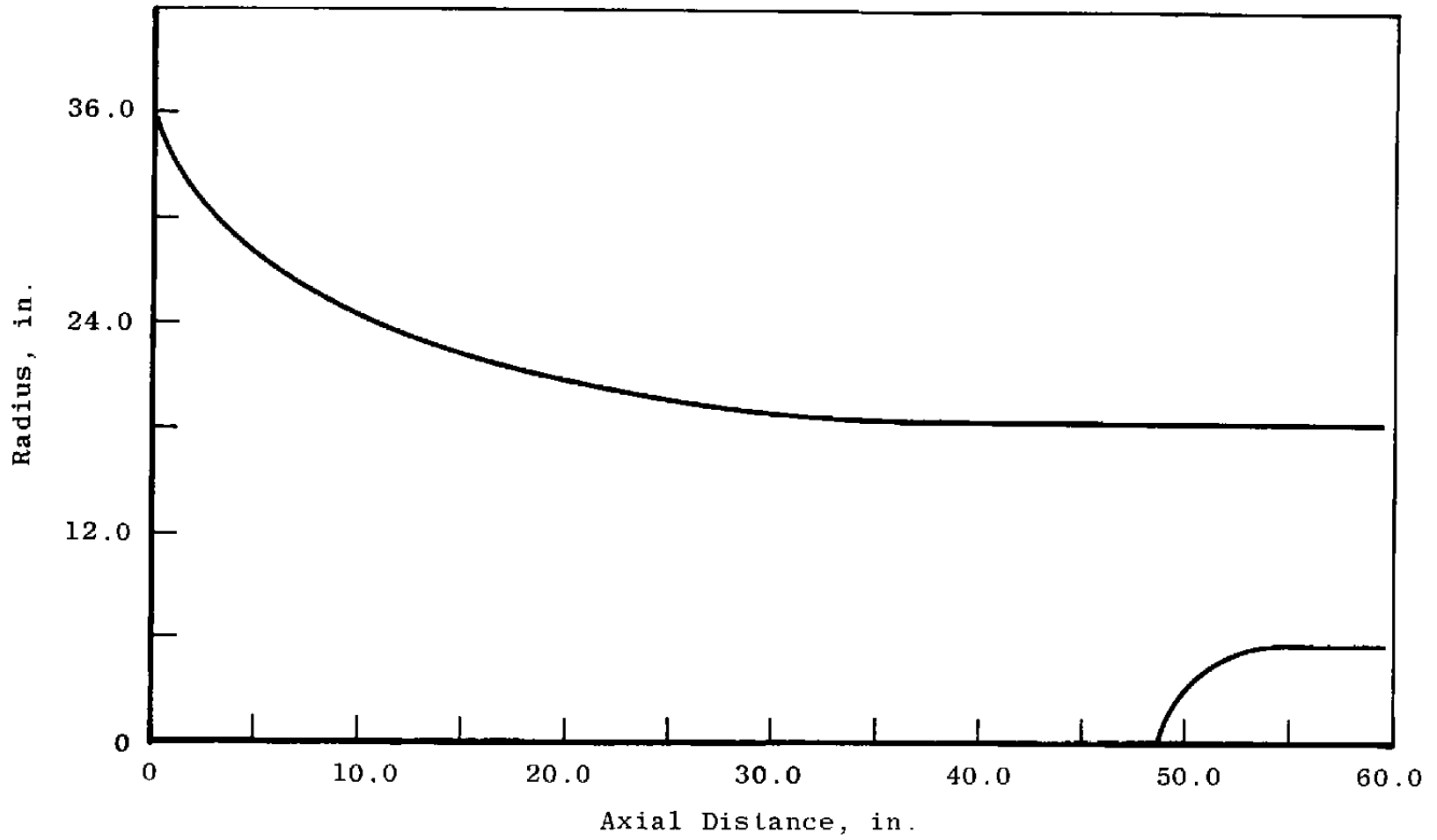
Figure 1. Preliminary engineering concept of TELS.



a. Inlet geometry A — NASA reference inlet  
Figure 2. Candidate inlet designs.



b. Inlet geometry B — straight cylindrical duct  
Figure 2. Continued.



c. Inlet geometry C – flared 2:1 ellipse  
Figure 2. Concluded.

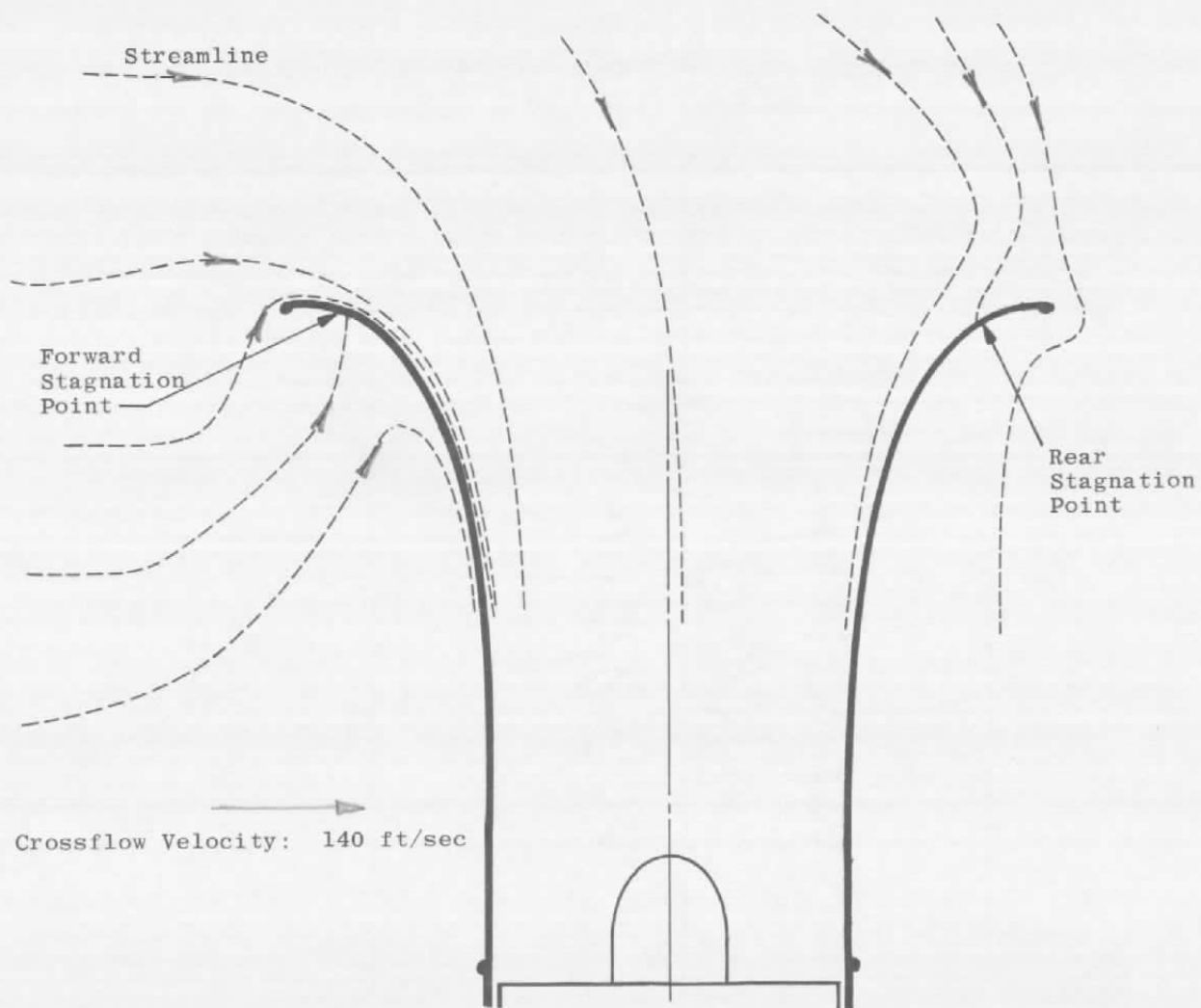
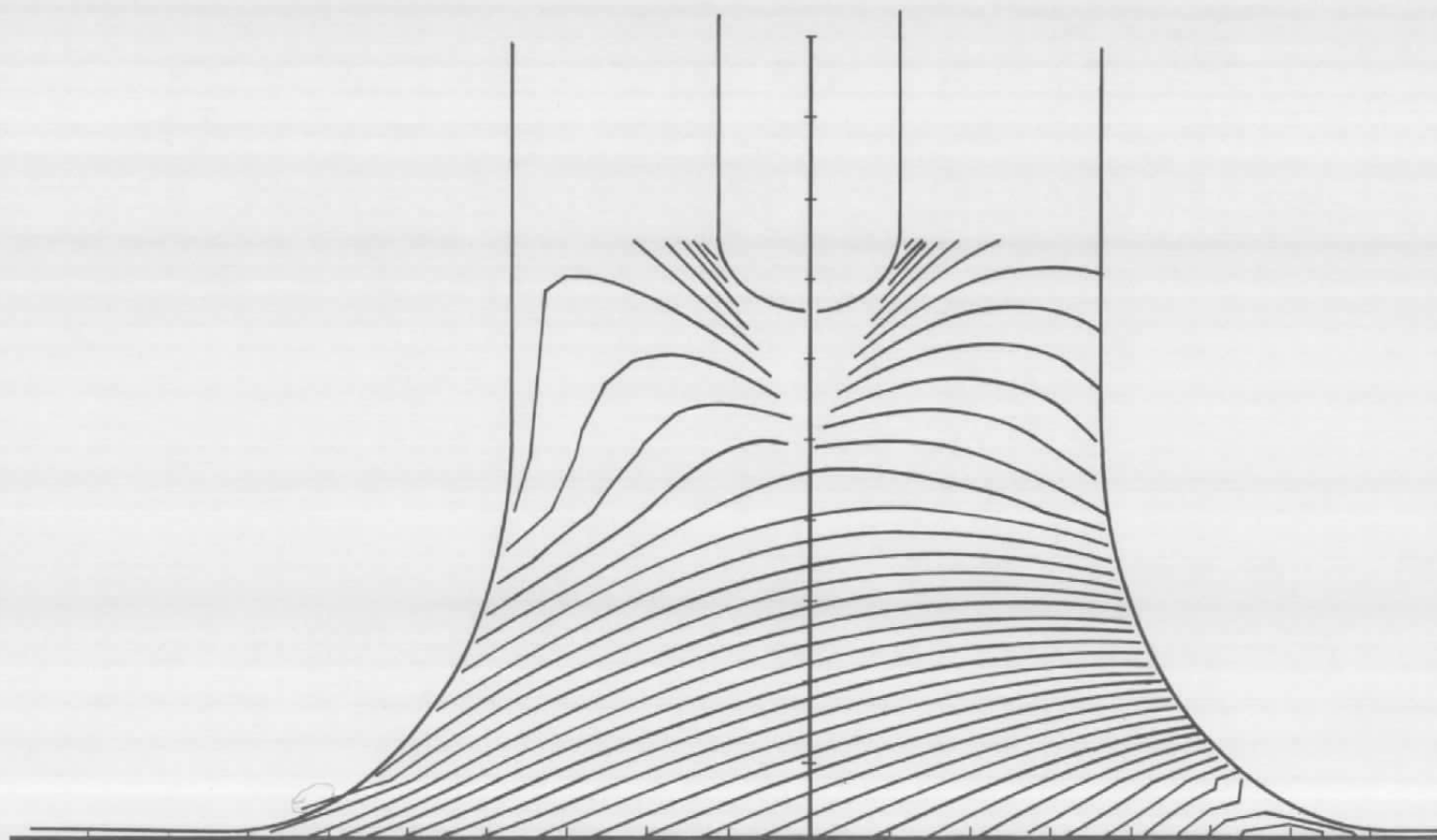


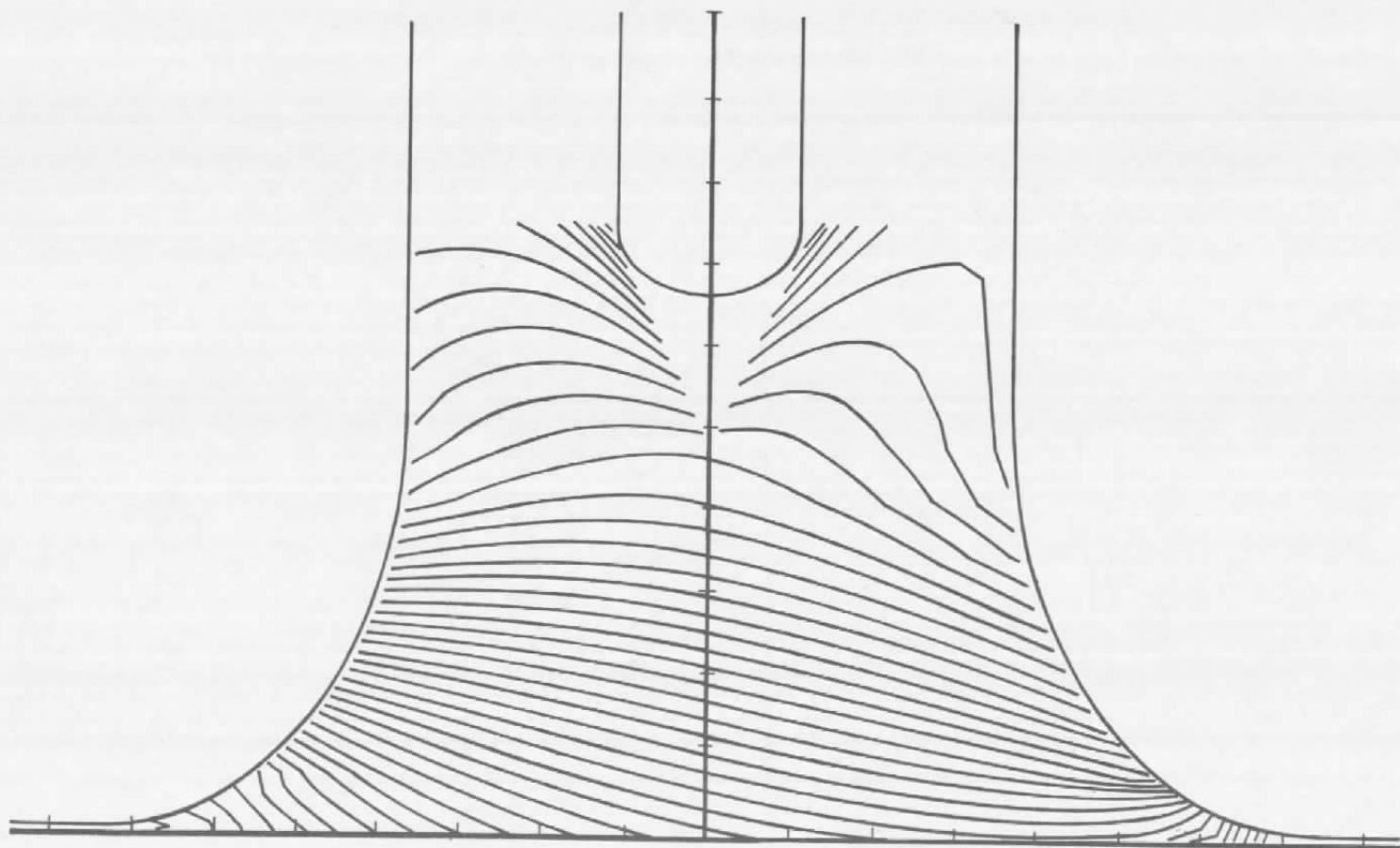
Figure 3. Approximate streamline pattern into flared bellmouth inlet, no inlet separation.



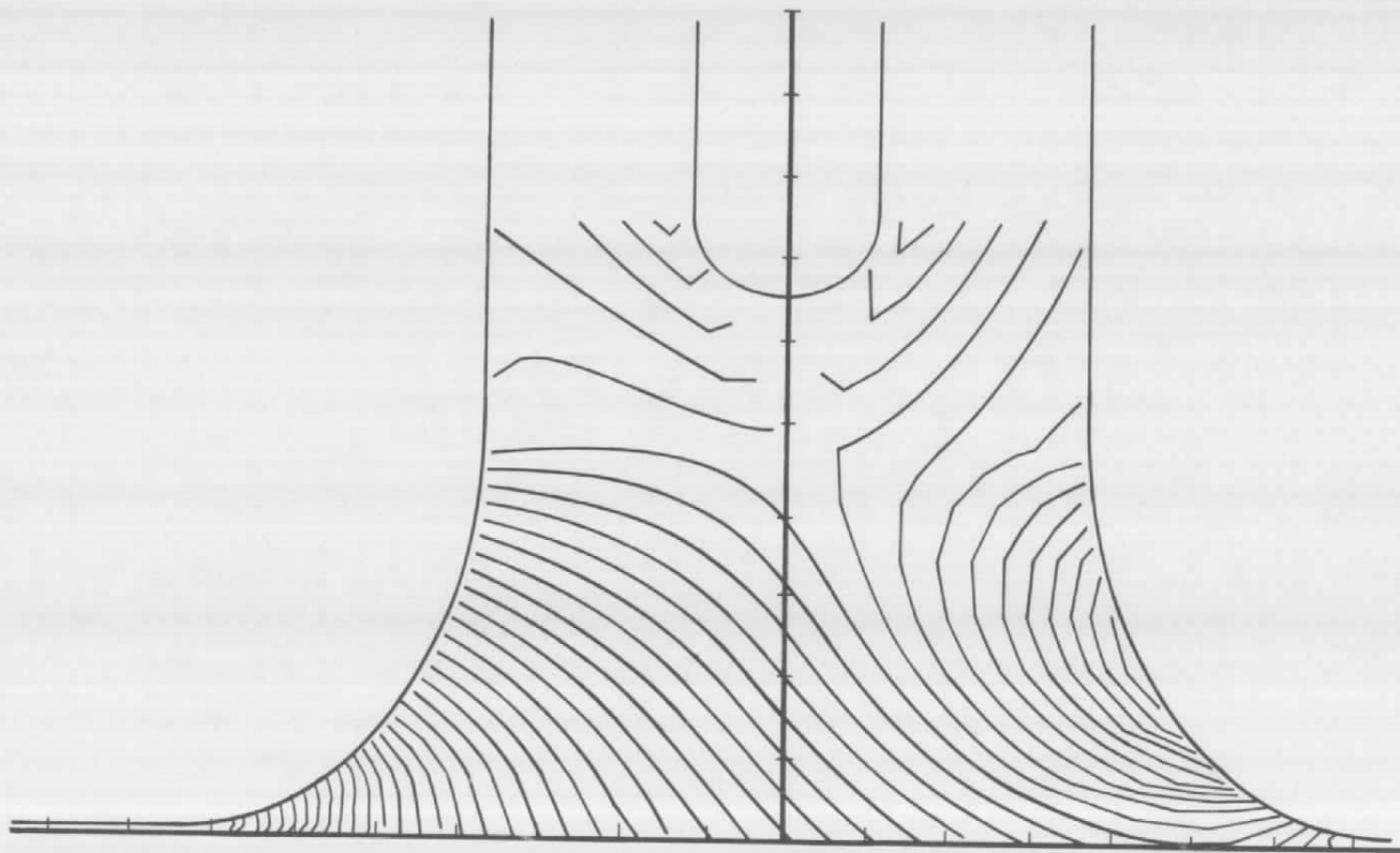
a. Lines of total velocity magnitude

Figure 4. Lines of isovelocity in meridional cross section of flared inlet showing nonuniformity of velocity field.

←  
Crossflow



b. Lines of axial velocity component  
Figure 4. Continued.



c. Lines of radial velocity component  
Figure 4. Concluded.

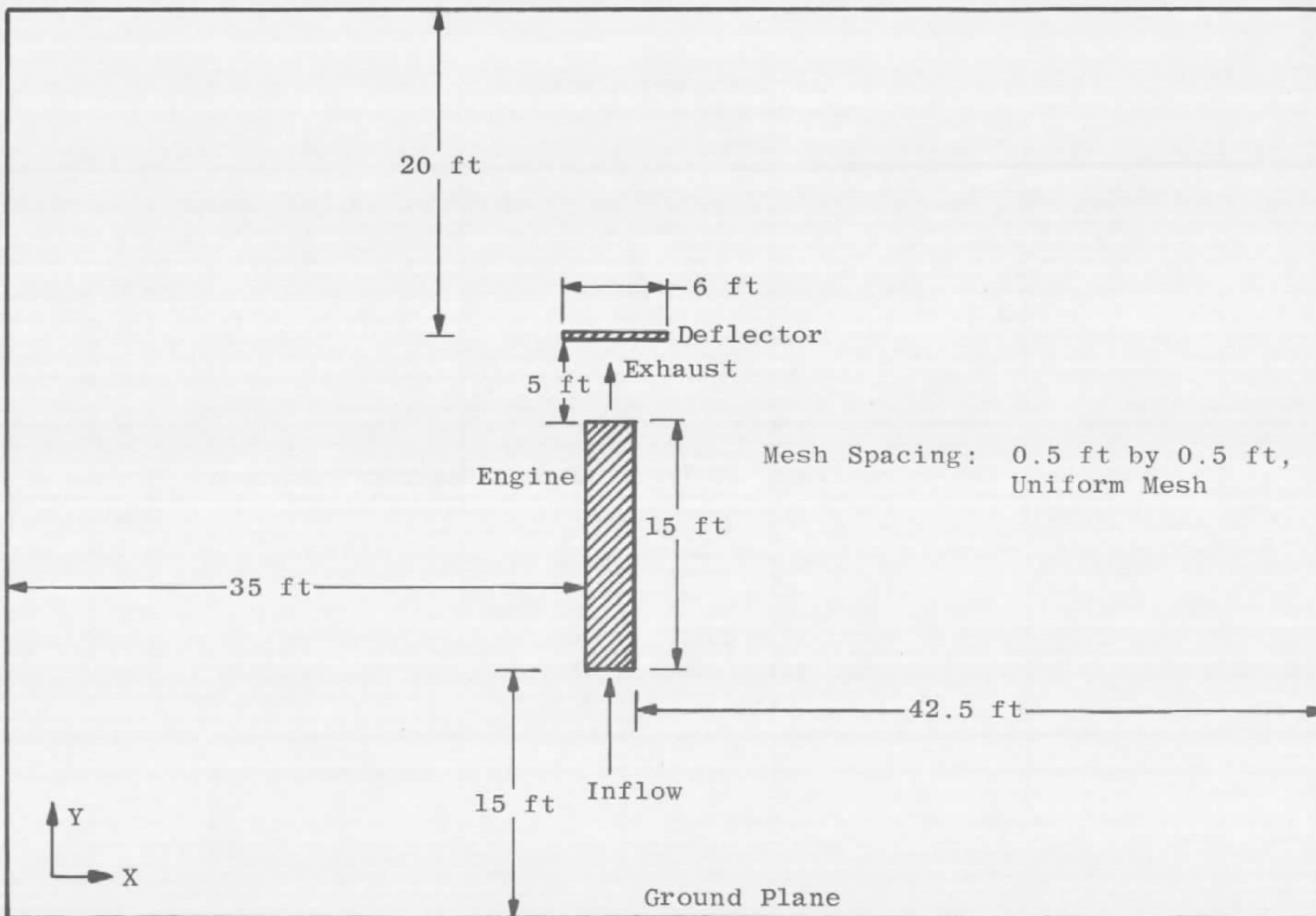
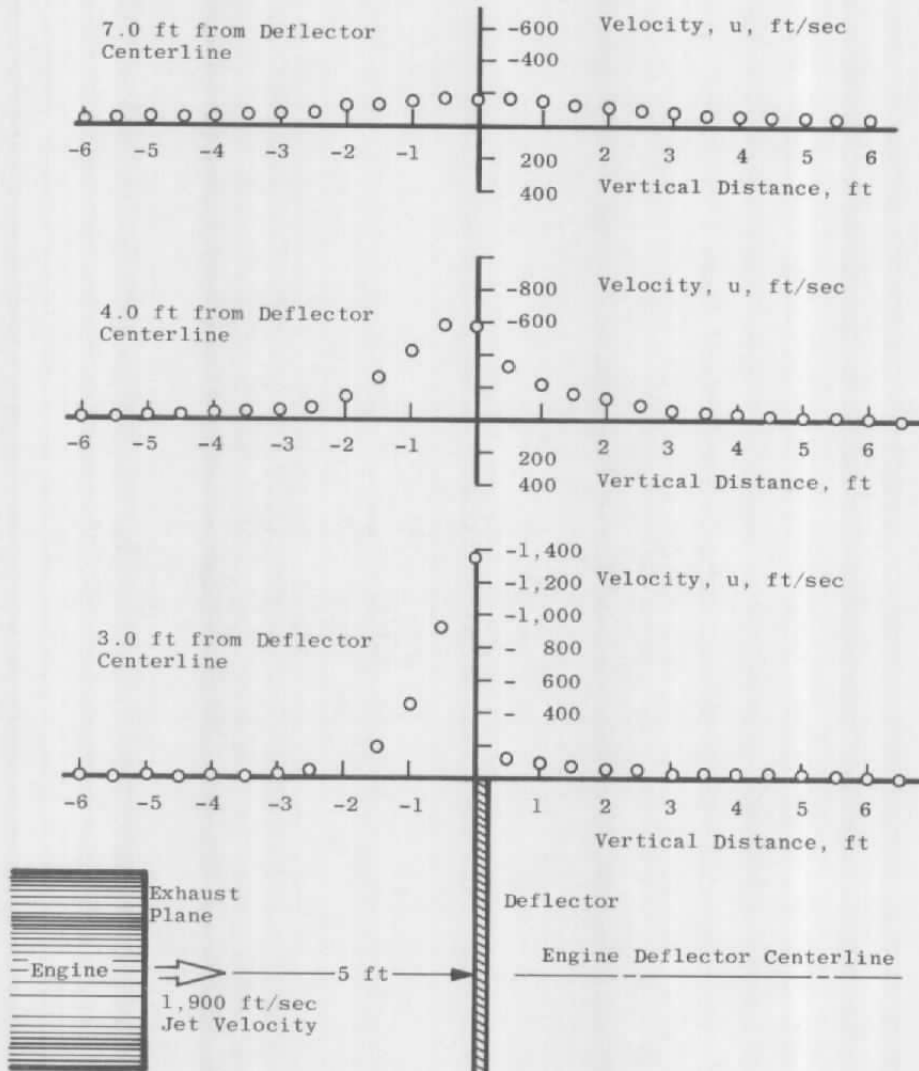
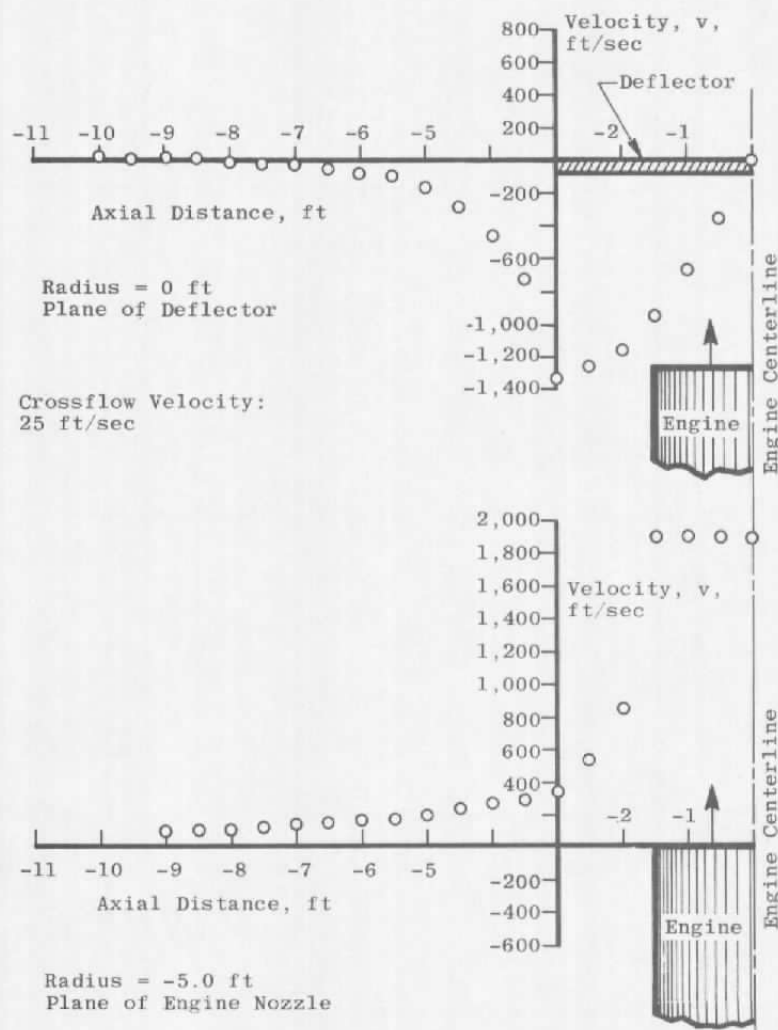


Figure 5. Schematic of engine and deflector simulation.

Turbulent Reynolds Number  
 $R_T = 2.2$  Based on  $b = 0.5$  ft  
 (see Appendix)  
 Crossflow Velocity: 25 ft/sec

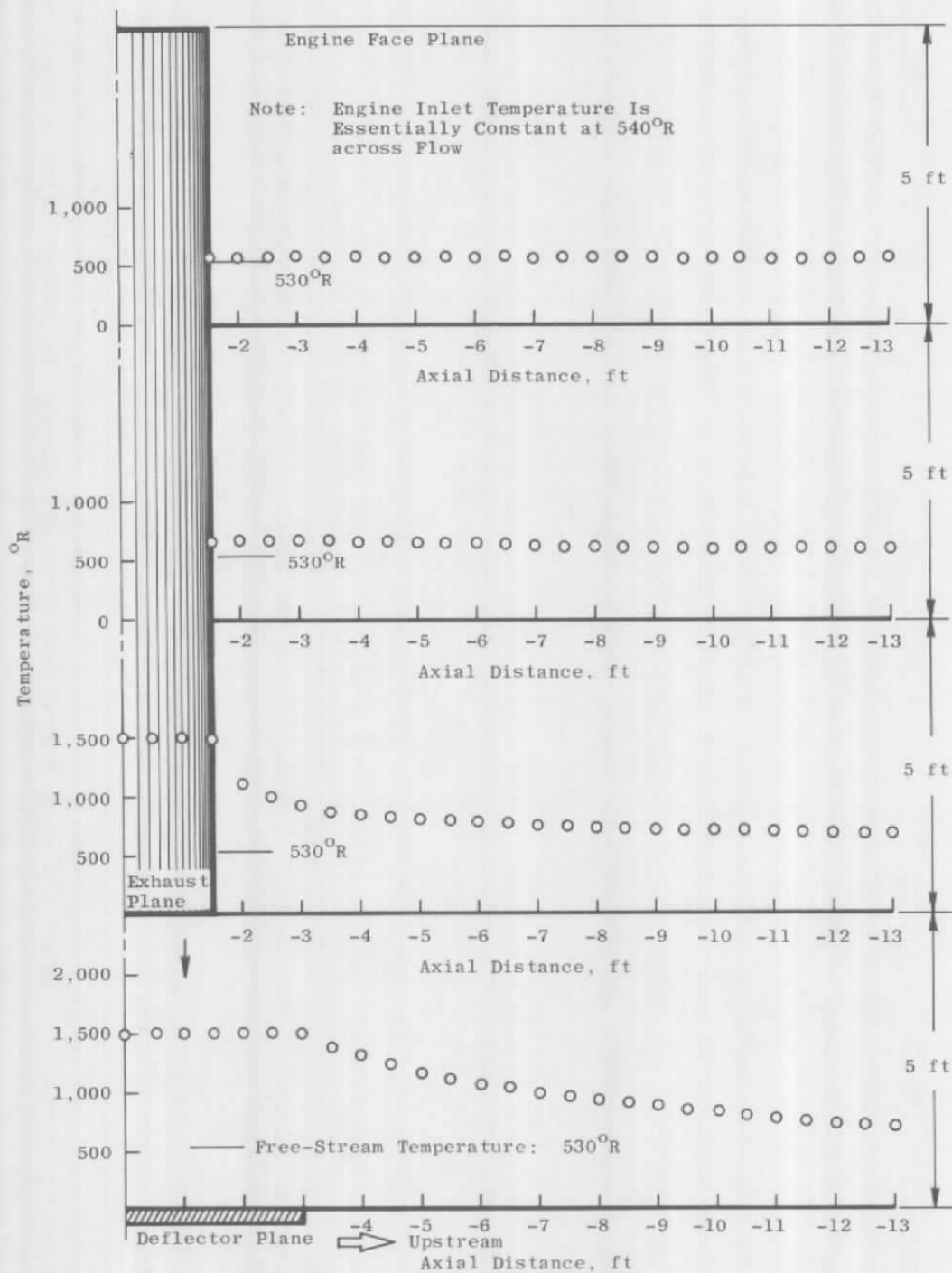


a. Profiles of axial velocity upstream of engine  
 Figure 6. Theoretical flow fields around the TELS  
 engine-exhaust deflector system.



b. Axial distribution of vertical velocity along two horizontal planes

Figure 6. Continued.



c. Profiles of free-stream temperature upstream of engine  
Figure 6. Concluded.

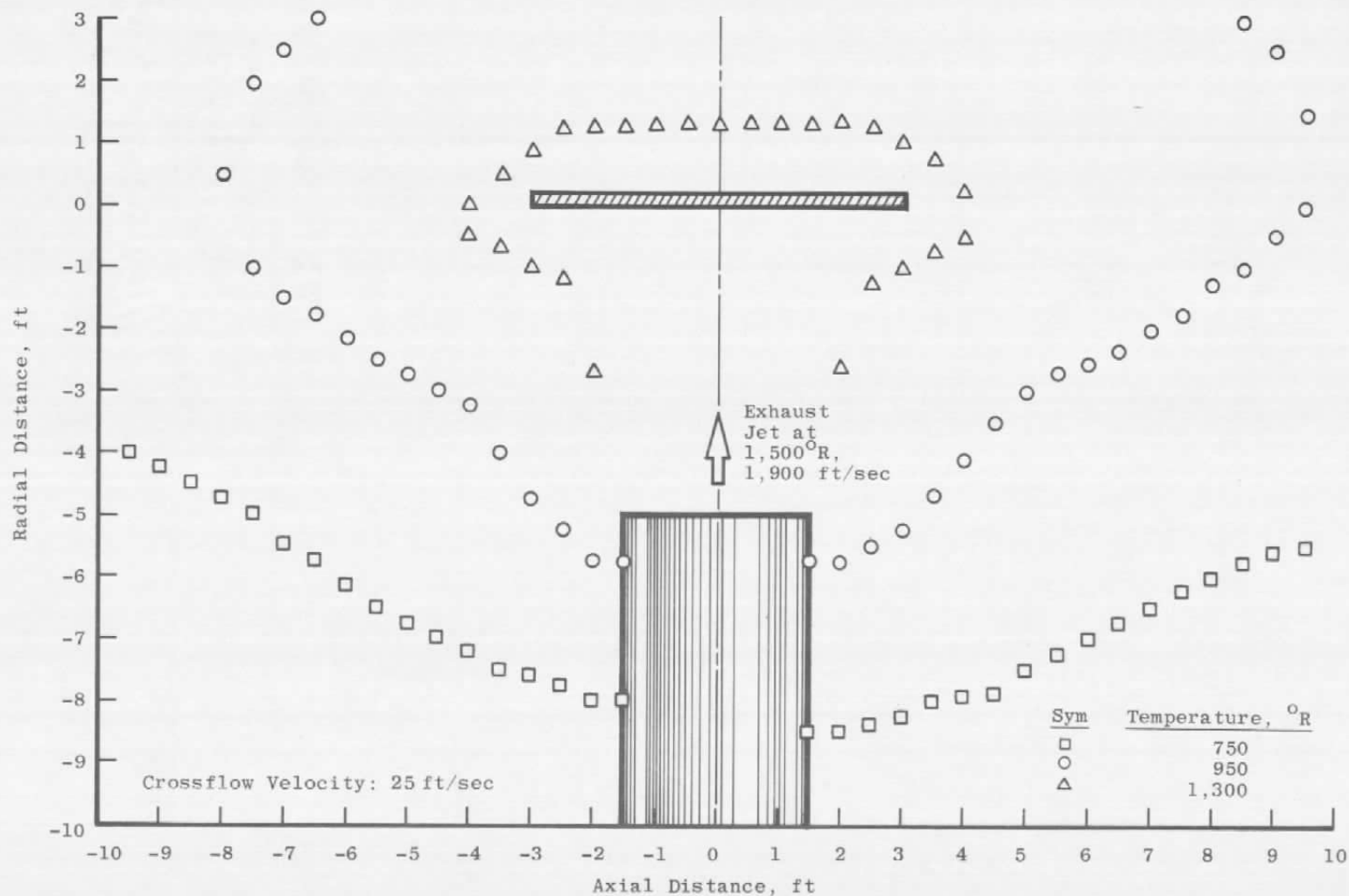


Figure 7. Isotherms around the engine-exhaust deflector system.

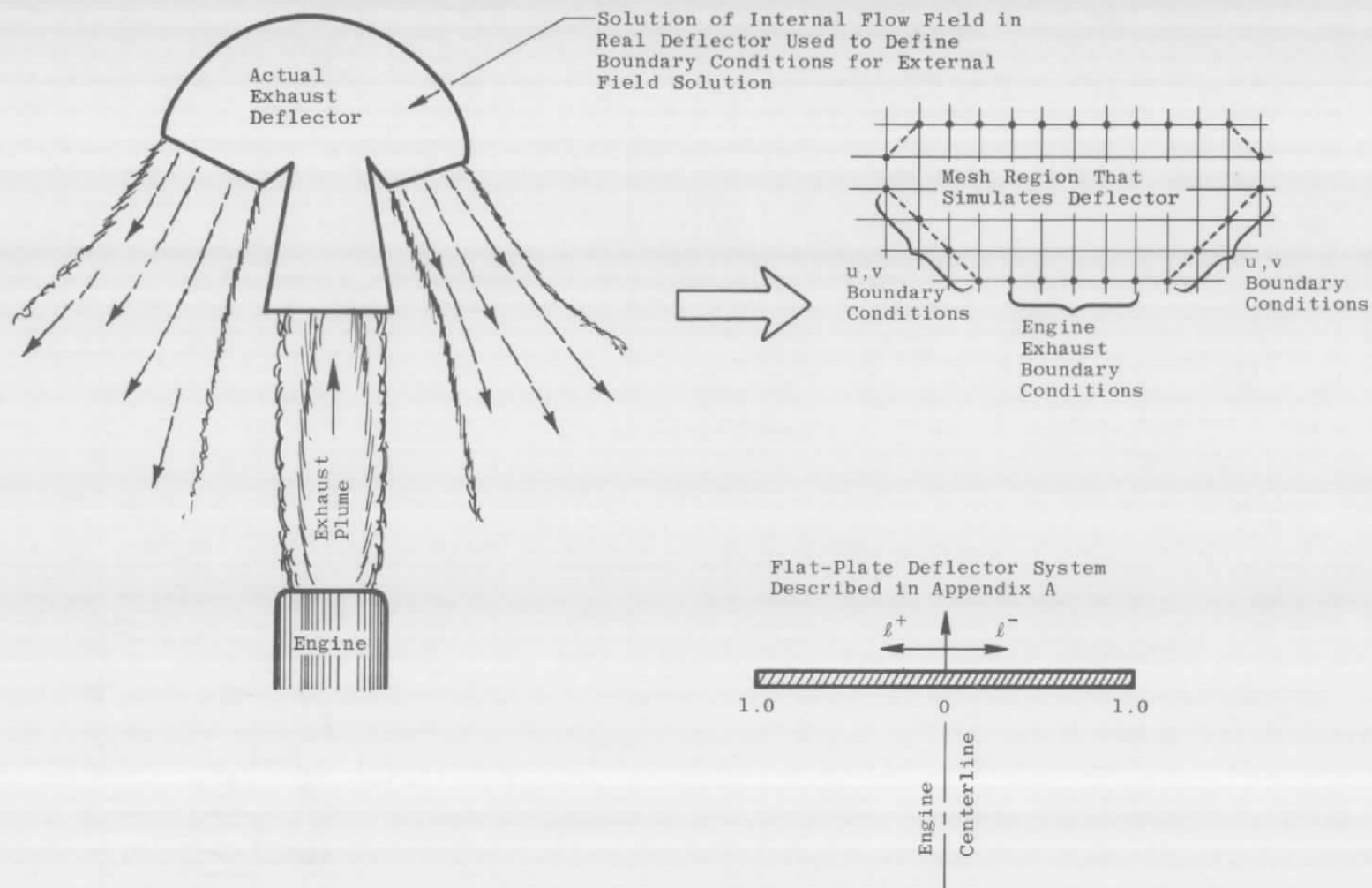


Figure 8. Models of exhaust gas deflectors.

**Table 1. Engine Mathematical Models at AEDC**

Engine Designation	In Current Use
J57-P-21/23	Yes
J75-P-17	Yes
YJ101-GE-100	No
TF30-P-3	Yes
TF30-P-7	No
TF30-P-100	Yes
TF33-P-7A	Yes
TF41-A-1	Yes
TF34-GE-100	No
F101-GE-100*	Yes
J85-GE-21	No
F100-PW-100*	Yes
J79-GE-15	Yes
TF39-GE-X	No
F107-WR-100	Yes

\*Indicates mathematical models known to include distortion indices.

## APPENDIX A

### COMPUTATIONS OF EXHAUST GAS INGESTION BY ENGINES IN TELS

#### A1.0 DESCRIPTION OF NUMERICAL SIMULATION OF GEOMETRY

The geometry simulated is a rectangular engine with a flat-plate jet deflector in a rectangular flow region. The engine is 3 ft wide and 15 ft long. The 6-ft-wide jet deflector is positioned 5 ft behind the engine. The flow region is 80 ft long and 55 ft high. The boundary conditions necessary for the computation are

Jet inlet velocity	400 fps
Jet exhaust velocity	1,900 fps
Jet exhaust temperature	1,500°R
Crossflow velocity	25 to 140 fps

The computational mesh is uniform and square with 0.5-ft spacings.

#### A2.0 SYSTEM OF GOVERNING EQUATIONS

These equations are for turbulent, incompressible, heated flows. The equations are the Navier-Stokes equations and the energy equation in plane, Cartesian coordinates.

##### A2.1 NAVIER-STOKES EQUATIONS

$$u \frac{\partial u}{\partial x} + v \frac{\partial u}{\partial y} = -\frac{1}{\rho} \frac{\partial p}{\partial x} + \nu_E \left[ \frac{\partial^2 u}{\partial x^2} + \frac{\partial^2 u}{\partial y^2} \right] \quad (\text{A2.1})$$

$$u \frac{\partial v}{\partial x} + v \frac{\partial v}{\partial y} = -\frac{1}{\rho} \frac{\partial p}{\partial y} + \nu_E \left[ \frac{\partial^2 v}{\partial x^2} + \frac{\partial^2 v}{\partial y^2} \right] - g \beta (\rho - \rho_\infty) \quad (\text{A2.2})$$

##### A2.2 ENERGY EQUATION

$$u \frac{\partial T}{\partial x} + v \frac{\partial T}{\partial y} = \frac{k_E}{\rho C_p} \left[ \frac{\partial^2 T}{\partial x^2} + \frac{\partial^2 T}{\partial y^2} \right] + \frac{\mu_E}{\rho C_p} \Phi_T \quad (\text{A2.3})$$

where the dissipation function is

$$\Phi_T = 2 \left[ \left( \frac{\partial u}{\partial x} \right)^2 + \left( \frac{\partial v}{\partial y} \right)^2 \right] + \left( \frac{\partial u}{\partial y} + \frac{\partial v}{\partial x} \right)^2 \quad (\text{A2.4})$$

## A2.3 PRESSURE EQUATION

For the pressure field, the Poisson's equation

$$\nabla^2 p = 2\rho \left[ \left( \frac{\partial u}{\partial x} \frac{\partial v}{\partial y} \right) - \left( \frac{\partial u}{\partial y} \frac{\partial v}{\partial x} \right) \right] = \Phi_p \quad (\text{A2.5})$$

given by Roache (Ref. 18) is solved. The density is related to the local pressure and temperature by

$$p = \rho RT$$

## A3.0 STANDARD FORM OF THE GOVERNING EQUATIONS

The equations are all rearranged in the form

$$a_{1\phi} \frac{\partial^2 \phi}{\partial x^2} + a_{2\phi} \frac{\partial^2 \phi}{\partial y^2} - b_{1\phi} \frac{\partial \phi}{\partial x} - b_{2\phi} \frac{\partial \phi}{\partial y} - d_\phi = 0 \quad (\text{A2.6})$$

The coefficients are listed below for each variable.

$\phi$	$a_{1\phi}$	$a_{2\phi}$	$b_{1\phi}$	$b_{2\phi}$	$d_\phi$
u	1	1	$u/v_E$	$v/v_E$	$-(1/\rho) \partial p / \partial x$
v	1	1	$u/v_E$	$v/v_E$	$-(1/\rho) \partial p / \partial y - g \beta (\rho - \rho_\infty)$
T	1	1	$u P_{r_E} / v_E$	$v P_{r_E} / v_E$	$(\mu_E / \rho C_p) \Phi_T$
p	1	1	0	0	$\Phi_p$

These equations are solved by the Chien "decay function" method of finite differences (Ref. 19). The continuity equation is not explicitly included in the governing set of equations; however, in the solution procedure, global checks on mass conservation are performed.

## A4.0 FINITE-DIFFERENCE SOLUTION PROCEDURE

The finite-difference method is point-by-point, Gauss-Siedel Relaxation of a system of algebraic equations of the form

$$\begin{aligned} \Phi_{i,j} = & C_{i+1,j} \Phi_{i+1,j} + C_{i-1,j} \Phi_{i-1,j} + C_{i,j+1} \Phi_{i,j+1} \\ & + C_{i,j-1} \Phi_{i,j-1} + D_{i,j} \end{aligned} \quad (\text{A2.7})$$

where  $C_{i,j}$  are the coefficients for the following five-point computational molecule:

$i+1,j$  = Eastern Node

$$C_{i+1,j} = C_E = \frac{(A1/\Delta X - B1/\Delta X)}{CR} \quad (A2.8)$$

$i-1,j$  = Western Node

$$C_{i-1,j} = C_W = \frac{(A1/\Delta X - B1/\Delta X)}{CR} \quad (A2.9)$$

$i,j+1$  = Northern Node

$$C_{i,j+1} = C_N = \frac{(A2/\Delta Y - B2/\Delta Y)}{CR} \quad (A2.10)$$

$i,j-1$  = Southern Node

$$C_{i,j-1} = C_S = \frac{(A2/\Delta Y - B2/\Delta Y)}{CR} \quad (A2.11)$$

where the A's and B's are

$$A1 = a_{1\phi}$$

$$A2 = a_{2\phi}$$

$$B1 = b_{1\phi}$$

$$B2 = b_{2\phi}$$

$$\Delta X = \Delta X$$

$$\Delta Y = \Delta Y$$

$$\Delta X = \Delta X$$

$$\Delta Y = \Delta Y$$

Finally, the CR parameter is calculated from the following:

$$CR = (2.0/\Delta X) + (2.0/\Delta Y) \quad (A2.12)$$

The point-wise source term,  $D_{i,j}$ , is as follows:

$$D_{i,j} = d_{\phi_{i,j}}/CR \quad (A2.13)$$

The decay functions,  $G_X$  and  $G_Y$ , are defined according to Chien (Ref. 19):

$$G_X = \begin{cases} 1 - 0.0625 R_X^2 & \text{if } |R_X| < 2 \\ \frac{2}{|R_X|} - \frac{1}{R_X^2} & \text{if } |R_X| \geq 2 \end{cases} \quad (A2.14)$$

$$GY = \begin{cases} 1 - 0.0625 R_y^2 & \text{if } |R_y| < 2 \\ \frac{2}{|R_y|} - \frac{1}{R_y^2} & \text{if } |R_y| \geq 2 \end{cases} \quad (A2.15)$$

$R_x$  and  $R_y$  are cell Reynolds numbers defined as

$$R_x = \frac{b_1 \Phi \Delta x}{a_1 \Phi} \quad (A2.16)$$

$$R_y = \frac{b_2 \Phi \Delta y}{a_2 \Phi}$$

## A5.0 TURBULENCE TRANSPORT THEORY

$\nu_E$  is an effective turbulent viscosity given by Schlichting (Ref. 20).

$$\nu_E = k_\mu V_{JET} R_{JET} = 0.0285 V_{JET} R_{JET} \quad (A2.17)$$

where  $V_{JET}$  and  $R_{JET}$  are the turbojet exhaust velocity and jet radius.

$P_{rE}$  is the effective turbulent Prandtl number defined as

$$P_{rE} = \frac{\mu_E C_p}{k_E} \quad (A2.18)$$

For most turbulent flows, experimentation gives  $0.6 \leq P_{rE} \leq 1.2$ . In the present study,  $P_{rE}$  was set to unity,  $P_{rE} = 1.0$ . The actual TELS operation is expected to induce much higher levels of turbulence and "mixing" than are given by the Schlichting formula for  $\nu_E$ . To simulate the high turbulence level induced by the TELS arm,  $\nu_E$  was increased by a factor of 10 in the numerical investigations, and the constant,  $k_\mu$ , was increased to 0.285 for some calculations. The results of these calculations are shown in Fig. 6.

## A6.0 MODELING TECHNIQUES FOR BOUNDARY CONDITIONS

The computer simulation solves a set of equations for  $u$ ,  $v$ ,  $T$ , and  $P$ , which are then specified on the boundaries of the region. These boundaries include the upstream, downstream, free-stream, and ground plane limits, plus the physical boundaries of the engine and deflector. The specific values assigned to these variables are as follows:

Upstream:  $u = U_{\infty}$  (crosswind velocity, ft/sec)  
 $v = 0$   
 $P = P$  (2116.0 psf)  
 $T = T_{\infty}$  (530°R)

Downstream:	Either	or
	$\partial u / \partial x = 0$	$u = U_{\infty}$
	$\partial v / \partial x = 0$	$v = 0$
	$P = P$	$P = P_{\infty}$
	$\partial T / \partial x = 0$	$T = T_{\infty}$

Free stream:  $u = U_{\infty}$   
 $v = 0$   
 $P = P_{\infty}$   
 $T = T_{\infty}$

Ground Plane:  $u = U_{\infty}$  (slip-velocity, neglecting the  
boundary layer)  
 $v = 0$   
 $\partial P / \partial y = 0$   
 $\partial T / \partial y = 0$

Engine:

Inlet:  $u = 0$   
 $v = 400$  ft/sec  
 $P = 2116.0$  psf  
 $\partial T / \partial y = 0$

Exhaust:  $u = 0$   
 $v = V_{JET}$  (1,900 ft/sec)  
 $T = 1,500^{\circ}R$   
 $P = 2116.0$  psf

$$\begin{aligned}
 \text{Sides:} \quad u &= 0 \\
 v &= 0 \\
 \partial T / \partial x &= 0 \\
 \partial P / \partial x &= 0
 \end{aligned}$$

$$\begin{aligned}
 \text{Deflector:} \quad & \underline{\text{along top surface}} \\
 u &= 0 \\
 v &= 0 \\
 T &= 1,500^\circ\text{R} \\
 \partial P / \partial y &= 0 \\
 & \underline{\text{along lower surface}} \\
 u &= u_d \text{ (ID, JD)} \\
 v &= v_d \text{ (ID, JD)} \\
 T &= 1,500^\circ\text{R} \\
 \partial P / \partial y &= 0
 \end{aligned}$$

The ability to model deflector geometry is provided through specifying the velocity  $u_d$ ,  $v_d$ , on the lower surface of the deflector. Thus, a velocity distribution is input to model the effects of a physical deflector. Methods exist for defining  $u_d$ ,  $v_d$  profiles (see, for example, Ref. 17). In the present study, the following functions were defined for  $u_d$  and  $v_d$ :

$$\begin{aligned}
 \text{Case 1} \quad u_d \text{ (ID, JD)} &= 0.0 \\
 v_d \text{ (ID, JD)} &= 0.0 \\
 \\
 \text{Case 2} \quad u_d \text{ (ID, JD)} &= -U_{\text{JET}}^* \sin\left(\frac{\pi}{2} \ell^+\right) \\
 u_d \text{ (ID, JD)} &= U_{\text{JET}}^* \sin\left(\frac{\pi}{2} \ell^-\right) \\
 v_d \text{ (ID, JD)} &= -V_{\text{JET}}^* \sin\left(\frac{\pi}{2} \ell^+\right) \\
 v_d \text{ (ID, JD)} &= V_{\text{JET}}^* \sin\left(\frac{\pi}{2} \ell^-\right)
 \end{aligned}$$

where the lengths  $\ell^+$ ,  $\ell^-$  are local normalized lengths along the deflector surface (Fig. 6). The velocities  $U_{\text{JET}}^*$  and  $V_{\text{JET}}^*$  are defined such that

$$V_{\text{JET}} = \sqrt{U_{\text{JET}}^{*2} + V_{\text{JET}}^{*2}}$$

## **A7.0 REMARKS ON THE OVERALL THEORY**

This numerical solution technique is a new approach to solving the Navier-Stokes equations directly by the application of existing theory. It has not been fully tested; only some preliminary calculations have been made for developing laminar boundary layers with and without heat transfer. Therefore, more research is required to assess the accuracy of this approach and to incorporate the pressure equation into the evolving solutions to examine the effects of compressibility on the jet deflection problem. Some standard flows — such as parallel jet mixing, turbulent pipe flows, and diffuser-type flows — should be computed and compared to existing numerical solutions and data. Because of the method's simplicity and broad applicability, it merits further investigation.

## NOMENCLATURE

$a_{1\phi}, a_{2\phi}$	Coefficients in the standard form of the governing equation [Eq. (A2.6)]
$b_{1\phi}, b_{2\phi}$	Coefficients in the standard form of the governing equation [Eq. (A2.6)]
$C_p$	Specific heat at constant pressure
$DX, DY$	Mesh spacings in the finite-difference simulation
$d_\phi$	Source terms in governing equations [Eq. (A2.6)]
$g$	Gravitational acceleration
$i, I$	Indices for mesh nodes in axial direction
$j, J$	Indices for mesh nodes in transverse direction
$k_L$	Effective thermal conductivity
$k_\mu$	Constant in viscosity function
$\xi^+, \xi^-$	Distances along deflector plate (Fig. 8)
$Pr_L$	Effective Prandtl number
$p$	Pressure
$R$	Radial Distance
$R_{JT}$	Turbojet exhaust jet radius
$T$	Temperature
$U_\infty$	Free-stream velocity
$U^*_{J T}$	Maximum x-direction velocity on deflector plate
$u$	x-direction velocity
$u_d$	x-direction velocity along deflector plate
$V_{J T}$	Turbojet exhaust jet velocity

$V_{1D,T}^*$	Maximum y-direction velocity along deflector plate
$v$	y-direction velocity
$v_D$	y-direction velocity along deflector plate
$x, X$	Axial direction
$y$	Transverse direction
$\beta$	Volume coefficient of thermal expansion
$\mu_T$	Effective dynamic viscosity
$\nu_T$	Effective kinematic viscosity
$\pi$	Pi (3.1415...)
$\rho$	Density
$\Phi_T$	Energy dissipation function